

Microarray based circRNA expression profiles in uremic plasma and PBMCs due to chronic glomerulonephritis

Xi Wang¹, Yong Dai², Wanfan Zhang¹, Donglin Sun³ and Xinzhou Zhang^{1,*}

¹ Department of Nephrology, The Second Clinical Medical College, Jinan University, Shenzhen People's Hospital, Shenzhen, Guangdong, 518000.

² Clinical Medical Research Center, The Second Clinical Medical College, Jinan University, Shenzhen People's Hospital, Shenzhen, Guangdong, 518000

³ Department of Urinary Surgery, Shenzhen Hospital of Southern Medical University, Shenzhen, 518100

*Corresponding author: zxinzhou1604@163.com

Received: May 20, 2016; Revised: July 19, 2016; Accepted: August 5, 2016; Published online: November 28, 2016

Abstract: Circular RNAs (circRNAs) have been identified in many diseases and shown to play important roles in pathological processes. The expression patterns of circRNA in uremia remains unknown. The aim of this study was to screen circRNA in plasma and peripheral blood mononuclear cells (PBMCs) in healthy controls and patients with uremia due to chronic glomerulonephritis, and to provide evidence for further exploration of the pathogenesis, diagnosis and treatment of uremic patients. Twenty individuals were included in this study, of which 10 were healthy and 10 were patients with uremia caused by chronic glomerulonephritis without systemic lupus erythematosus (SLE). Peripheral blood was collected from each individual in the two groups and the PBMCs were separated. The circRNAs expression profile was examined using a human circRNA microarray. The expression of differently expressed circRNAs was further validated by qRT-PCR. Seven hundred ten circRNAs were differentially expressed in the plasma in the two groups, accounting for 27.58% of the total circRNA (710/2578). Three hundred eighty-five upregulated circRNAs accounted for 14.93% and 325 downregulated circRNAs accounted for 12.60% of the total circRNAs. Additionally, 968 circRNAs were differentially expressed in PBMCs in the two groups, accounting for 29.24% of all circRNAs (968/3310). Six hundred seventy upregulated circRNAs accounted for 20.24% and 298 downregulated circRNAs accounted for 9.00% of the total circRNAs. The results of qRT-PCR validation were consistent with the microarray gene expression results. The expression profile of circRNAs was altered in the plasma and PBMCs of patients with uremia, which suggests that the changed circRNAs may be potential diagnostic biomarkers that play an important role in the pathogenesis of uremic patients. We speculate that *hsa_circ_0053958*, *hsa_circ_0103281* may be associated with the pathogenesis of uremia and may be potential biological molecular markers for the diagnosis and prognosis of uremia.

Key words: uremia; glomerulonephritis; PBMCs; circular RNAs; microarray

INTRODUCTION

In addition to the classic tRNAs, mRNAs and rRNAs, cells contain additional RNA types, such as micro RNAs (miRNAs), long noncoding RNAs (lncRNAs), small interfering RNAs (siRNAs), and other noncoding RNAs. A growing component of this family of diverse RNA molecules are circular RNAs (circRNAs) [1]. CircRNAs are a special class of endogenous RNAs featuring stable structure and high tissue-specific expression. Compared to linear RNAs, circRNAs have the remarkable characteristic of non-canonical splic-

ing without a free 3' or 5' end [2], and are mainly composed of exons which are widespread in the mammalian genome. In recent years, with the rapid development and widespread application of RNA sequencing, researchers have found that many exonic transcripts can form circRNAs through nonlinear reverse splicing or gene rearrangement. Moreover, circRNAs account for a large proportion of all spliced transcripts [2]. Both exonic and intronic circRNAs have potential functions in the regulation of gene expression. It has been reported that circRNA can function as sponge adsorption (miRNA sponge), which antagonizes mi-

croRNAs (miRNAs) to inhibit the expression of their target genes to benefit mRNAs that escape miRNA regulation at the transcriptional level [3]. More recently, other functions, such as interfering pre-mRNA splicing [4], which serves as a template for protein synthesis [5] and the regulation of parental genes [6], have also been reported.

Chronic glomerulonephritis (CGN), or nephritis for short, is one of the most severe kidney diseases, and it is characterized by basic clinical manifestations including proteinuria, hematuria, hypertension, gout and edema [7]. CGN is a common clinical syndrome, and the incidence rate in China is approximately 0.4% [8]. It may occur at any age, presenting an insidious onset that is mild to severe, with varying degrees of renal dysfunction, repeated protracted illness, and slow progressive development that eventually leads to chronic renal failure (CRF) called uremia.

CircRNAs have been identified in colorectal cancer, ovarian cancer [9] and gastric cancer [10]. Researchers have established that circRNAs are highly stable in mammalian cells and that one specific circRNA, hsa_circ_002059, may be a potential novel and stable biomarker for the diagnosis of gastric carcinoma [10]. Qin et al. [11] found that hsa_circ_001649 was significantly downregulated in hepatocellular carcinoma (HCC) and indicated that it might serve as a novel potential biomarker for HCC and function in HCC tumorigenesis and metastasis. A global reduction in circular RNA abundance in colorectal cancer cell lines and cancer compared with normal tissues has been reported, revealing a negative correlation between global circular RNA abundance and proliferation [12]. However, few studies have reported results for uremia or other kidney diseases, and little is known about the expression profile of circRNAs related to the pathogenesis of uremia.

The aim of this study was to characterize the differences in differential expression of circRNAs in chronic glomerulonephritis-induced uremic patients and healthy persons based on circRNA microarray technology, and to attempt to provide evidence that circRNAs can function as a diagnostic marker or therapeutic target for the diagnosis and treatment of uremia.

MATERIALS AND METHODS

Ethics statement

All participants gave their informed consent prior to inclusion in the study. All studies were approved by the Institute Research Medical Ethics Committee of Shenzhen People's Hospital.

Patients

Demographic data and physiological characteristics are provided in Table 1. Briefly, 20 people from the

Table 1. Demographic data and physiological characteristics of patients (n=10)

Item	Patients
Age (years)	54.60±18.08
Gender	6 Males, 4 Females
Height (cm)	168±6.94
Body weight (kg)	65.50±10.72
Blood pressure (mmHg)	91.40±11.27/15.90±13.18
Urinary protein excretion (g/24h)	2.13±0.86
GFR (ml/min/1.73 ²)	7.00±3.83
Serum potassium (mmol/L)	4.89±0.74
Serum Calcium (mmol/L)	2.14±0.16
Serum phosphate (mmol/L)	1.89±0.46
Hemameba (10 ⁹ /L)	6.75±1.43
Erythrocyte (10 ¹² /L)	3.77±1.32
Thrombocyte (10 ⁹ /L)	170.60±64.15
Hemoglobin (g/L)	112.40±39.16
CO ₂ -CP (mmol/L)	20.79±4.77
Uric Acid (mmol/L)	521.10±109.69
Cystatin(mg/L)	3.70±1.28
IgG1(g/L)	5.62±1.43
IgG2 (g/L)	3.10±0.59
IgG3 (g/L)	0.59±0.36
IgG4 (g/L)	0.81±0.26
C3(g/L)	1.00±0.22
C4 (g/L)	0.30±0.06
IgA (g/L)	3.04±1.23
IgG(g/L)	11.17±3.15
IgM (g/L)	0.87±0.65
serum albumin (g/L)	35.87±2.97
urea nitrogen (mmol/L)	26.55±8.33
serum creatinine (umol/L)	892.2±353.12
parathyroid hormone (pg/ml)	580.02±546.49
25-(OH)D (ng/ml)	14.9±4.12
urine protein (g/L)	2.73±1.76
urine pH	6.15±1.11
albumin/creatinine (mg/g)	2236.19±917.86

Shenzhen People's Hospital of Nephrology were included in this study; the profile of clinical features, pathological changes and renal ultrasonography were used to classify the patients with chronic glomerulonephritis, among which 10 uremic patients were hospitalized from November to December in 2014 and comprised 4 females and 6 males with an age range from 31-68 years old (average age: 54.60 ± 18.08). The inclusion criteria were: i) patients with clinical symptoms, including nausea and vomiting, chest tightness, shortness of breath, difficulty breathing, renal hypertension and edema, and ii) a glomerular filtration rate less than 15 mL/min, (3) renal ultrasound with cortical thinning and renal atrophy, in accordance with the standard of morphology changes in chronic kidney disease (CKD). The exclusion criteria were: (i) other kidney disease; (ii) allergic purpura nephritis and lupus nephritis; (iii) elevated anti-o and plasma C3 levels that returned to normal within 4 to 8 weeks. All patients met the kidney disease: improving global outcomes (KDIGO) standards, and blood samples were collected prior to drug treatment and renal replacement therapy. Ten cases of normal healthy control subjects from the same period were enrolled from among the employees of Shenzhen People's Hospital, excluding those employees with high blood pressure, heart disease, diabetes, autoimmune diseases or other diseases; the resultant group of healthy controls comprised 4 females and 6 males ranging in age from 23 to 58 years old (average age: 39.81 ± 12.13).

Sample collection

Peripheral blood (4 mL) was collected into vacuum tubes, and plasma samples were isolated by centrifugation at $2000 \times g$ for 10 min at room temperature (EDTA and citrate were used to prevent blood coagulation). PBMCs were isolated from the peripheral blood of 10 uremia patients and 10 healthy controls according to the method of Kuo et al. [13].

RNA isolation and cRNA microarray analysis

Total RNA was isolated using Trizol[®] reagent (Invitrogen, USA). The quality and concentration of the RNA were determined using a NanoDrop ND-1000 spectrophotometer (NanoDrop Technologies, Wilm-

ington, USA, $A260/280 > 2.0$; $A260/230 > 1.8$). The RNA integrity was assessed by 1% wt/vol denaturing agarose gel electrophoresis using GelRed dye. The RNA samples were treated with RNase Rand DNase I (Epicenter Technologies, Madison, WI) to remove linear RNAs and contaminating genomic DNA.

Hybridization of RNA microarrays

Each sample was amplified and transcribed into fluorescent cRNA along the entire length of the transcripts without 3' bias, utilizing a random priming method. The cRNA was labeled using an Arraystar Super RNA Labeling Kit (Arraystar, Rockville, MA, USA), according to the manufacturer's protocol. The labeled cRNA was then purified using the RNeasy Mini Kit (Qiagen, USA). The hybridization solution for each sample was prepared using a Gene Expression Hybridization Kit (Agilent, USA) and 1.5 μg of the Cy3-labeled cRNA was hybridized using an Agilent Human circRNA Microarray (6x7K, Arraystar, USA) for 17 h at 65°C. The slides were subsequently washed, dried and scanned using a GenePix 4000B axon microarray scanner (Axon Instruments Inc, CA, USA).

Collection and analysis of circRNA microarray data

GenePix Pro 6.0 software (Axon) was used for grid alignment and data extraction. The raw data from the array images were then extracted using Feature Extraction software version 11.0.1.1 (Agilent, USA), and quantile normalization of the raw data and subsequent data processing were performed using the R software package. Differentially expressed circRNAs between the two groups were analyzed using the Student t-test. Significantly differentially expressed circRNAs (fold changes ≥ 2.0 and p-values ≤ 0.05) between the two groups were identified by Volcano Plot filtering. Hierarchical clustering analysis was performed using Pearson's correlation to display the distinguishable circRNA expression patterns among samples. The circRNA-microRNA interaction was predicted with Arraystar's homemade miRNA target prediction software, and all the differentially expressed circRNAs were annotated in detail with the circRNA-miRNA interaction information.

Quantitative real-time PCR analysis

Based on the circRNA microarray results, twelve differentially expressed circRNAs were selected for quantitative real-time PCR validation. The mRNA expression levels of hsa_circRNA_0044922, hsa_circRNA_0037409, hsa_circRNA_0004951, hsa_circ_0049271, hsa_circ_0053958, and hsa_circ_0000369 in plasma, and hsa_circ_0102750, hsa_circ_0101521, hsa_circ_0101364, hsa_circ_0103281, hsa_circ_0102682 and hsa_circ_0102075 in PBMCs, were further validated by quantitative real-time PCR. Briefly, total RNA was isolated from plasma using an RNeasy Mini Kit (Qiagen, USA). cDNA was synthesized using the Maxima First Strand cDNA Synthesis Kit from Thermo Fisher (USA) according to the manufacturer's protocol. Quantitative real-time PCR was performed using Absolute Blue QPCR SYBR Green ROX mix from Thermo Scientific, on an Applied Biosystems Step One Plus real-time system. The primer sequences for real-time quantitative PCR are shown in Table 2.

Statistical analysis

The relative expression level of differentially expressed circRNAs is presented as the means \pm SD. One-way analysis of variance (ANOVA) was used for analysis within the two groups. $P < 0.05$ was considered statistically significant.

RESULTS

Experimental design and workflow

To detect the expression profile of circRNAs in plasma and PBMC, a microarray-based approach was used for screening and for comparison of the expression patterns between the uremia patients with the healthy control group. The experiments workflow is shown in Fig. 1. Total RNA was isolated from the plasma and PBMCs of the healthy and the uremia groups and used for microarray hybridization; the RNA was labeled with Cy3 fluorescent dye marker (green), the labeled RNA was purified and then hybridized with Arraystar Human circRNA microarray.

Table 2. Primer database for real-time quantitative PCR.

Name	Primers	Product length (bp)
β -actin (plasma)	F:5' GTGGCCGAGGACTTTGATTG3'	73
	R:5' CCTGTAAACAACGCATCTCATATT3'	
hsa_circ_0044922	F:5' CCCTTCACCTTCGCTATCAAAC3'	174
	R:5' CACAGGCGCATATCTTCTCTTT3'	
hsa_circ_0037409	F:5' CTCTATTCTCTCAGGAACCTCGCC3'	75
	R:5' CGGACGCACAGCAGACAGAT3'	
hsa_circ_0004951	F:5' GTTACAACCTGGAGCCTGGATT 3'	167
	R:5' AACACCTGACGAGTTGCTGAC 3'	
hsa_circ_0049271	F:5' ACTTCGCTGAGCAGATTGGC3'	125
	R:5' GCATGGGGTTCCAGAAGATAAG3'	
hsa_circ_0053958	F:5' GTGTGAGACAGAGGTGTGCC3'	148
	R:5' GCAGCCAGCAATAAGGTTTTC3'	
hsa_circ_0000369	F:5'ACCTCAGTTACCTCAGGAAAGA3'	76
	R:5' CTCCTGACGCTGAGTCAAAGA3'	
β -actin (PBMC)	F:5' GTGGCCGAGGACTTTGATTG3'	73
	R :5'CCTGTAAACAACGCATCTCATATT3'	
hsa_circ_0102750	F:5' CATCTAACACACCCTTACCCTTC3'	106
	R:5' ACTGTTGTCCAAGCCATACC3'	
hsa_circ_0101521	F:5' GTTACAACCTGGAGCCTGGATT3'	167
	R:5' AACACCTGACGAGTTGCTGAC3'	
hsa_circ_0101364	F:5' ATCCATGTGACCATGAGGAAA3'	136
	R:5'TCTGTGAGAACCATAACAAAACCA3'	
hsa_circ_0103281	F:5' CAACAATTCCTGGCGATACCT 3'	121
	R:5' GTCATAGATTTCTCCACGGCTC3'	
hsa_circ_0102682	F:5' CCTGCCCTTCTGTATCCTGTG3'	136
	R:5' TTGCAGCCAGCAATAAGGTTT3'	
hsa_circ_0102075	F:5'' GTGCAACAACCTGGCAAGGC3'	135
	R:5' ATCTGTGTTGCCATCATTTTACC3'	

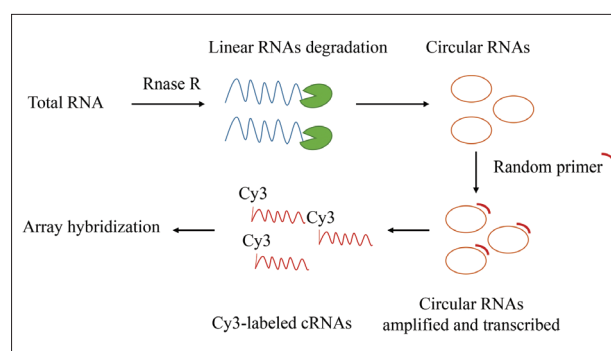


Fig. 1. Experimental workflow of the microarray expression profiles of circular RNAs.

Hybridization analysis

The hybridization mixture was applied to a glass gas- ket, and with the microarray was scanned with an Axon GenePix 4100A Scanner and analyzed with GenePix Pro 6.0 software. The final analysis outputs

are shown in Fig. 2A, demonstrating that the fluorescent signal was evenly distributed and with a low signal-to-noise ratio.

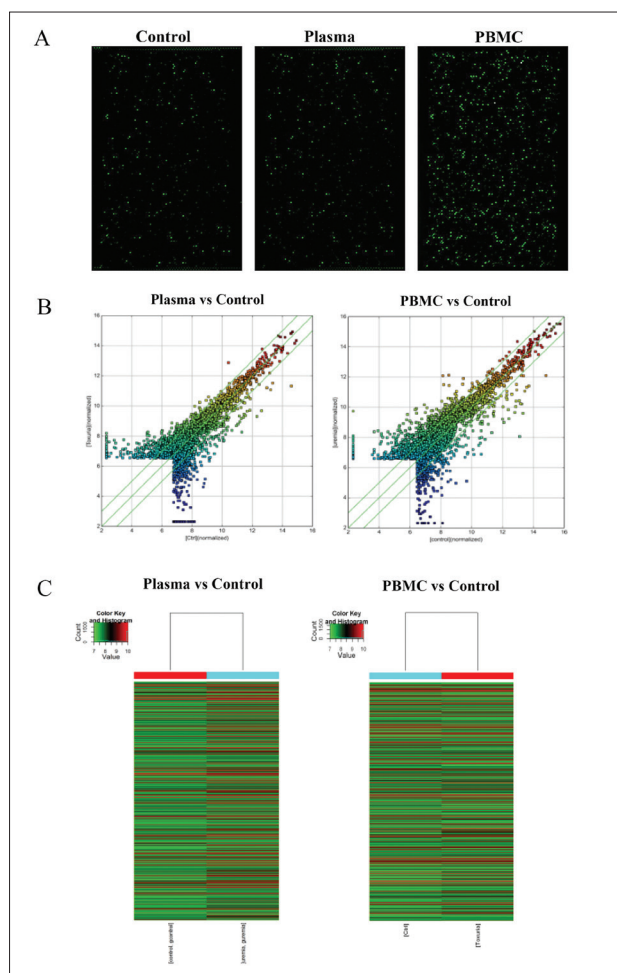


Fig. 2. **A** – Fluorescent analysis output of the hybridization mixture. The hybridization mixture was applied to the glass gasket, scanned with the Axon GenePix 4100A Scanner, and analyzed with GenePix Pro 6.0 software. The fluorescent signal was evenly distributed with a low signal-to-noise ratio. **B** – Scatter plot used to assess variation in circRNA expression in the two groups. The values obtained for the X and Y axes in the scatter plot are the normalized signal values determined for the samples (log₂ scaled) or the average normalized signal values obtained for the groups of samples (log₂ scaled). The green lines represent the fold change. The circRNAs above the top green line and below the bottom green line indicate a change greater than 2-fold in the circRNAs in the two groups. **C** – Heat map clustering of 710 986 circRNAs expressed in the plasma and PBMCs. Clustering was performed using Cluster 3.0 software. The colors in the map display the relative values of all tiles within two groups. Red represents upregulated and green represents downregulated circRNAs. The brightness of the color indicates the degree of up- or downregulation.

Scatter plot of the log average difference in circRNA expression

The scatter plot revealed overlapping circRNA expression profiles of the plasma and PBMCs. The values obtained for the X and Y axes in the scatter plot are the normalized signal values of the samples (log₂ scaled) or the averaged normalized signal values of groups of samples (log₂ scaled). The green lines are fold change lines. The circRNAs above the top green line and below the bottom green line indicated more than 2-fold change of circRNAs between the two compared samples (Fig. 2B).

Hierarchical cluster analysis of differential circRNA expression

Hierarchical clustering was performed based on “All Targets Value - CircRNAs” using plasma and PBMCs from the healthy control group and the uremic patient group. The hierarchical clustering results revealed distinct circRNAs expression profiles between the two groups (Fig. 2C).

Microarray-based analysis of circRNA expression in plasma between patients with uremia and healthy controls

As shown in Fig. 3A, 710 circRNAs were differentially expressed in the plasma in the two groups, accounting for 27.58% of the total circRNAs (710/2578). Of these, 385 circRNAs were upregulated, accounting for 14.93% of the total circRNAs, and 325 circRNAs were downregulated, accounting for 12.60%. The expression of hsa_circ_0006602 showed the most dramatic increase (fold change = 58.62); the expression of hsa_circ_0062317 showed the most dramatic decrease (-57.12 fold change).

Microarray-based analysis of circRNA expression in PBMCs in patients with uremia and healthy controls

Additionally, 968 circRNAs were identified as differentially expressed in the PBMC in the two groups, accounting for 29.24% of the total circRNAs (968/3310), of which 670 circRNAs differentially expressed were upregulated, accounting for 20.24%; 298 differentially

Table 3. The most significantly expressed of 20 upregulated and 20 downregulated circRNA in plasma.

circRNA	Fold change	Regulation	chromosomal location	gene symbol
hsa_circ_0006602	58.6178506	up	chr1	SRSF4
hsa_circ_0091104	50.7178506	up	chrX	ATRX
hsa_circ_0004951	50.4178506	up	Chr15	TRPM7
hsa_circ_0004245	50.4178506	up	Chr13	TDRD3
hsa_circ_0001095	48.4678506	up	Chr2	PLEKHM3
hsa_circ_0008057	48.0178506	up	Chr1	EYA3
hsa_circ_0001517	43.5678506	up	Chr5	FBXL17
hsa_circ_0038072	41.8178506	up	Chr16	ABCC1
hsa_circ_0018031	40.9178506	up	Chr10	MASTL
hsa_circ_0072391	34.73798	up	Chr5	HMGCS1
hsa_circ_0087283	32.6178506	up	Chr9	TLE4
hsa_circ_0004312	32.3178506	up	Chr7	AP4M1
hsa_circ_0002884	30.7178506	up	Chr11	PICALM
hsa_circ_0000169	30.5678506	up	Chr1	NEK7
hsa_circ_0068481	30.5678506	up	Chr3	ST6GAL1
hsa_circ_0026911	30.3678506	up	Chr12	RNF41
hsa_circ_0011168	29.7543658	up	Chr1	EPB41
hsa_circ_0047444	29.7178506	up	Chr18	MOCOS
hsa_circ_0092330	29.4178506	up	Chr22	ARVCF
hsa_circ_0068894	29.0178506	up	Chr4	WHSC1
hsa_circ_0062317	-57.1178506	down	chr8	ZFAT
hsa_circ_0001818	-52.0178506	down	chr8	UBR5
hsa_circ_0079619	-51.4178506	down	chr7	MPP6
hsa_circ_0008305	-47.9178506	down	chr8	PTK2
hsa_circ_0062937	-42.3178506	down	chr22	PRR14L
hsa_circ_0011692	-36.9178506	down	chr1	STK40
hsa_circ_0018909	-34.6178506	down	chr10	VDAC2
hsa_circ_0055412	-32.8178506	down	chr2	CAPG
hsa_circ_0012967	-31.1678506	down	chr1	RABGGTB
hsa_circ_0049888	-31.1678506	down	chr19	EPS15L1
hsa_circ_0047378	-30.0178506	down	chr18	RNF138
hsa_circ_0092341	-29.2178506	down	chr6	C6orf132
hsa_circ_0013339	-28.8178506	down	chr1	SLC30A7
hsa_circ_0046188	-28.8178506	down	chr17	NPLOC4
hsa_circ_0022812	-26.8178506	down	chr11	POLA2
hsa_circ_0008910	-26.1178506	down	chr4	DCTD
hsa_circ_0001666	-25.2178506	down	chr6	FAM120B
hsa_circ_0004294	-25.0373255	down	chr22	EIF3L
hsa_circ_0067913	-25.0178506	down	chr3	PHC3
hsa_circ_0077527	-24.8178506	down	chr6	BVES

expressed circRNAs were downregulated, accounting for 9.00%. Hsa_circ_101364 and hsa_circ_104694 showed the most marked up- and downregulated circRNAs, respectively. We ranked the circRNAs according to fold change (FC) in expression levels, and a complete list of the top 20 candidates of up- or down-

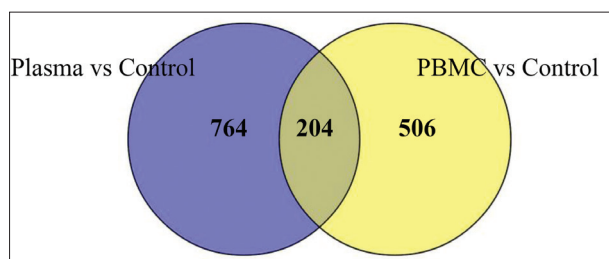


Fig. 3. Venn Diagram which provides a specialized view for capturing commonalities between differentially expressed circRNAs. Two hundred four circRNAs (12.15% (204/1679)) were differentially expressed in the plasma and PBMCs; 506 circRNAs (30.14% (506/1679)) were only differentially expressed in plasma, while 764 circRNAs (45.50% (764/1679)) were only have differentially expressed in PBMCs.

regulated circRNAs are provided in Tables 2 and 3, including the respective circRNA names, fold change, regulation, chromosomal location and gene symbol.

Common differentially expressed circRNAs in plasma and PBMCs

A Venn diagram for the differentially expressed circRNAs in the plasma and PBMCs is shown in Fig. 3. Two hundred four common circRNAs were differentially expressed in the plasma and the PBMC, accounting for 12.15% (204/1679) of the total circRNAs, of which 113 were upregulated and 91 were downregulated. Five hundred six circRNAs were only differentially expressed in plasma (30.14% (506/1679)), while 764 circRNAs (45.50% (764/1679)) were only differentially expression in PBMCs.

miRNA binding sites of circRNAs

The circRNA/microRNA interaction was predicted with Arraystar's homemade miRNA target prediction software based on Target Scan and miRanda. We discovered that several microRNA were related to circRNAs (Table 4). Presumably, a number of different microRNA binding sites are present on circRNAs, thus regulating the microRNA target gene in a multitude of ways.

Quantitative real-time PCR validation

The microarray mRNA expression levels of hsa_circ_0044922, hsa_circ_0037409, hsa_circ_0004951, hsa_circ_0049271, hsa_circ_0053958, hsa_

Table 4. The most significantly expressed of 20 upregulated and 20 downregulated circRNAs in PBMC.

circRNA	Fold change	Regulation	Chromosomal location	Gene symbol
hsa_circ_101364	171.1735687	up	chr14	HIF1A
hsa_circ_104809	55.3735687	up	chr9	UBQLN1
hsa_circ_100100	50.2735687	up	chr1	TMEM50A
hsa_circ_102962	45.4735687	up	chr2	NDUFA10
hsa_circ_104256	42.1735687	up	chr6	SYTL3
hsa_circ_103704	36.7735687	up	chr4	PDLIM5
hsa_circ_101996	34.8735687	up	chr17	SPECC1
hsa_circ_001959	34.1735687	up	chr5	—
hsa_circ_104875	33.1735687	up	chr9	SUSD1
hsa_circ_100772	32.7735687	up	chr11	KIF18A
hsa_circ_101875	32.2735687	up	chr16	RFWD3
hsa_circ_101974	30.2735687	up	chr17	EIF4A1
hsa_circ_104792	28.3735687	up	chr9	GNAQ
hsa_circ_100627	28.0735687	up	chr10	VCL
hsa_circ_103466	28.0735687	up	chr3	RAB7A
hsa_circ_100052	27.1735687	up	chr1	PLOD1
hsa_circ_102343	25.8681915	up	chr18	RNF138
hsa_circ_100984	24.9735687	up	chr11	FOXRED1
hsa_circ_101475	24.9735687	up	chr15	THBS1
hsa_circ_100288	24.5735687	up	chr1	CDC14A
hsa_circ_104694	-55.3735687	down	chr8	ZFAT
hsa_circ_104670	-38.5735687	down	chr8	UBR5
hsa_circ_100647	-33.284837	down	chr10	EXOC6
hsa_circ_100457	-29.1735687	down	chr1	KCTD3
hsa_circ_001689	-24.7735687	down	chr19	—
hsa_circ_100177	-23.8737637	down	chr1	STK40
hsa_circ_102101	-23.8556673	down	chr17	CDC27
hsa_circ_102774	-22.9735687	down	chr2	CAPG
hsa_circ_000689	-22.7735687	down	chr2	—
hsa_circ_400081	-21.9735687	down	chr4	—
hsa_circ_101786	-18.0735687	down	chr16	EIF3CL
hsa_circ_102444	-18.0735687	down	chr19	DNM2
hsa_circ_101660	-16.657577	down	chr15	ASB7
hsa_circ_101998	-16.0472568	down	chr17	SPECC1
hsa_circ_104166	-26.8178506	down	chr11	POLA2
hsa_circ_103972	-26.1178506	down	chr4	DCTD
hsa_circ_101006	-25.2178506	down	chr6	FAM120B
hsa_circ_103890	-25.0373255	down	chr22	EIF3L
hsa_circ_103599	-25.0178506	down	chr3	PHC3
hsa_circ_100077	-24.8178506	down	chr6	BVES

circ_0000369 in plasma and hsa_circ_0102750, hsa_circ_0101521, hsa_circ_0101364, hsa_circ_0103218, hsa_circ_0102682 and hsa_circ_0102075 in PBMCs were further validated by quantitative real-time PCR. The results are shown in Fig. 4. The expression levels of hsa_circ_0037409, hsa_circ_0004951 and hsa_circ_0053958 in plasma were significantly higher than

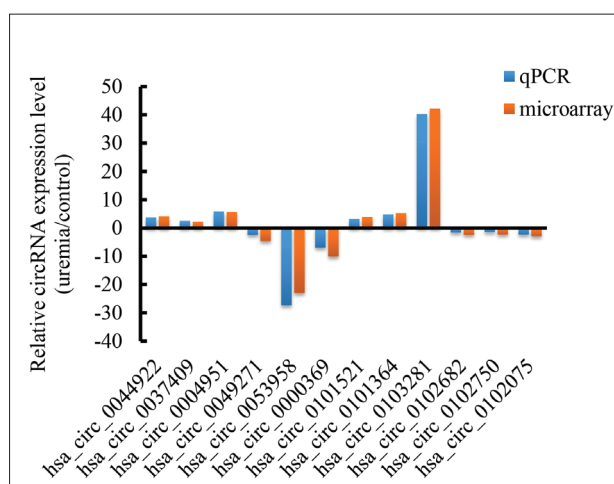


Fig. 4. Microarray mRNA expression levels of hsa_circ_0044922, hsa_circ_0037409, hsa_circ_0004951, hsa_circ_0049271, hsa_circ_0053958, hsa_circ_0000369 in plasma and hsa_circ_0102750, hsa_circ_0101521, hsa_circ_0101364, hsa_circ_0103281, hsa_circ_0102682 and hsa_circ_0102075 in PBMCs were further validated by quantitative real-time PCR.

those in the control. The expression levels of hsa_circ_0101521, hsa_circ_0101364, hsa_circ_0103218, and hsa_circ_0102075 in PBMCs were significantly higher than those in the control.

DISCUSSION

Uremia is the state of ill health resulting from renal failure, and chronic glomerulonephritis is still the most frequent cause of irreversible renal failure, which is associated with numerous complications. Currently available drugs can delay the onset of kidney failure or slow-down the progression of uremia, but there are still no clear methods to prevent or reverse uremia at the molecular or genetic level. Therefore, an improved understanding of the pathogenesis of uremia is required. Renal fibrosis is the final pathology of patients with uremia. In recent studies, it has been reported that the severity of renal tubulointerstitial injury is the most important factor involved in the prognosis of uremia. Therefore, the prevention and reduction of renal tubulointerstitial injury during early disease stages and delayed progression of chronic conditions to reduce or eliminate renal fibrosis are the most important steps in kidney disease prevention and control. Concurrently, uremia can lead to features of complicated symptoms, including disorders in nutrition metabolism, cardio-

vascular disease, anemia, electrolyte disorders, skeletal myopathy, endocrine dyspraxia and respiratory disorders. The biochip is one of the main advantages of the genomic revolution, and it has been used to screen for various diseases by evaluating miRNA targeting of mRNAs and differential expression of genes, proteins and microRNAs to assess biological functions and understand the disease pathology.

In the present work, we compared the differential expression of circRNAs in plasma and PBMCs of healthy controls with that of patients with uremia due to chronic glomerulonephritis, to identify potential diagnostic and treatment markers of uremia. Out of 710 screened circRNAs, a total of 968 were observed to be significantly differentially expressed in plasma leukocytes and PBMCs in patients with uremia due to chronic glomerulonephritis, as judged by microarray. The differentially expressed circRNAs were further validated by qRT-PCR. These differences in gene expression were mainly related to biological functions, including cell differentiation, mutation, deletion, activation, homeostasis, motility, signal transduction, immune responses and other features such as AP4M1, RNF41, ST6GAL1, TRPM7, WDR37, RNF138, PSEN1, PPP2R5A and Notch. For example, Notch is closely related to proteinuria/glomerular sclerosis and renal function. Laura et al. [14] found that the severity of glomerular disorders depends on the Notch-regulated balance between podocyte death and regeneration provided by renal progenitors. Murea et al. [15] found that cleaved Notch1, Notch2 and Jagged1 are expressed on podocytes in proteinuric nephropathies and that their expression levels correlate with the amount of proteinuria across all disease groups. The degree of glomerulosclerosis was found to correlate with the podocyte expression of cleaved Notch1, while the severity of tubulointerstitial fibrosis and the estimated glomerular filtration rate correlated with the expression of cleaved Notch1 in the tubulointerstitium. Sassi et al. [16] used exome sequencing data to rapidly screen rare coding variability in PSEN1 and PSEN2 in a British cohort composed of 47 unrelated early-onset Alzheimer's disease cases and 179 healthy controls, and the results suggested that PSEN1 plays an important role in the nervous system.

In the present study, we found that 710 circRNAs were differentially expressed in the plasma of the two

groups, accounting for 27.58% of the total circRNA. The hsa_circ_0006602 and hsa_circ_00062617 were clearly increased or decreased in the plasma, and the hsa_circ_0101364 and hsa_circ_0104694 were increased or decreased in PBMCs; these results were related to SRSF4, ZNF74, HIF-1 α , and ZFAT. Serine/arginine-rich splicing factor 4 (SRSF4) is essential for pre-mRNA splicing and can influence the selection of the alternative splice site. SRSF4 plays an important role in the regulation of G1 to S phase cell cycle progression and in the alternative splicing of HIPK2 during tumor growth, and SRSF4 downregulation induces apoptosis in colon cancer cells [17]. Zinc finger protein 74 (ZNF74) encodes an RNA-binding protein that is tightly associated with the nuclear matrix. Kim et al. [18] reported that the Gli subfamily Krüppel-like zinc finger protein Glis2 is essential for the maintenance of normal renal functions, and a deficiency in Glis2 expression leads to tubular atrophy and progressive fibrosis similar to nephronophthisis, ultimately resulting in renal failure. Hypoxia inducible factor-1 α (HIF-1 α) has been shown to play a role in the pathogenesis of renal interstitial fibrosis, and the intensity of HIF-1 α renal expression plays a role in the pathogenesis of chronic kidney disease [19].

Recent studies showed that circRNA has some characteristics that are mainly present in the cytoplasm and to a lesser extent in the nucleus [20], such as a closed ring, structural stability [21], no poly-A tail structure, no recognition or decomposition by nuclease [2,22], and the presence of elements acting by miRNA sponge adsorption that regulate gene expression at the transcriptional level [23]. Moreover, circRNAs can function as miRNA sponges or regulators of parent gene expression that affect disease initiation and progression. CircRNAs are widely expressed in human cells, and their expression levels can be 10-fold or higher compared to their linear isomers [2]. The most two important properties of circRNAs are highly conserved sequences and a high degree of stability in mammalian cells [23]. Compared with other noncoding RNA, such as miRNAs and lncRNAs, these properties provide circRNAs with the potential to become ideal biomarkers in the diagnosis of uremia. Our results suggest that hsa_circ_0021110, hsa_circ_0006148, hsa_circ_0091074, hsa_circ_0006686, hsa_circ_0103362 and hsa_circ_010362618 are associated with microRNA-141. HIPK2 is the target gene of miR-141 and is

involved in renal interstitial fibrosis. Additionally, the expression of HIPK2 can be regulated by miR-141. We found that the expression of such circRNAs related to miRNAs increased significantly and could promote expression of the HIPK2 gene to aggravate renal fibrosis and to promote uremia. Hsa_circ_0064584 and the other downregulated circRNAs were associated with miR-24, which participates in vascular endothelial cell (VEC) proliferation and apoptosis, angiogenesis, inflammatory reactions and the expression of miR-24, which is positively associated with the severity of hypertension and complications [24]. Hsa_circ_0000854, hsa_circ_0101753, hsa_circ_0000854 and the other 35 differentially expressed circRNAs are predicted to be associated with miRNA-146a, which can enhance the expression of TNF- α , TGF- β 1 and NF- κ B and promote renal interstitial fibrosis and related atherosclerosis [25,26]. Recently, several studies reported that miRNAs play important roles in autoimmune diseases, and Lu et al [27] found that intrarenal miR-638, miR-198 and miR-146a are differentially expressed in peripheral blood and urine of patients with lupus nephritis compared to healthy controls. Furthermore, the degree of change in glomerular miR-146a and tubulo-interstitial miR-638 expression correlated with clinical disease severity. The Notch signal transduction pathway is

closely related to proteinuria, glomerular sclerosis and renal function [14,15]; the transient receptor potential cation channel, subfamily M, member 7 (TRPM7) gene is constitutively expressed in mammalian heart, liver, lung, kidney, gastrointestinal tract, brain and bones. Protein phosphorylation, phosphatidylinositol 4,5-bisphosphate or PtdIns(4,5)P₂ (PIP₂) activation, G_q proteins which participate in cellular signaling pathways, divalent cations play important roles in ischemia-reperfusion and regulate the electrolyte balance inside and outside of cells [28], thus affecting ring finger protein 138 (RNF138) gene [29] and the presenilin-1 (PSEN1) gene in the nervous system [30], among others.

Current research suggests that circRNA through microRNA sponge adsorption antagonizes miRNA to inhibit the expression of its target genes, thus enhancing target gene expression. The association of miRNA with various diseases has been confirmed, and circRNA is also closely related to the development of disease. CircRNA/miRNA interaction was predicted using Arraystar's homemade miRNA target prediction software based on Target Scan [31] and miRanda [32]. We identified several miRNAs related to circRNAs (Table 5). Presumably, a number of different miRNA

Table 5. miRNA binding sites of circRNAs.

circRNA	Regulation	microRNA binding sites				
hsa_circ_0025395	up	hsa-miR-608	hsa-miR-30b-3p	hsa-miR-330-5p	hsa-miR-638	hsa-miR-138-5p
hsa_circ_0003152	up	hsa-miR-1301-3p	hsa-miR-130b-5p	hsa-miR-204-3p	hsa-miR-29b-1-5p	hsa-miR-877-3p
hsa_circ_0037078	up	hsa-miR-223-3p	hsa-miR-875-3p	hsa-miR-148b-5p	hsa-miR-92a-2-5p	hsa-miR-665
hsa_circ_0001119	up	hsa-miR-623	hsa-miR-622	hsa-miR-328-5p	hsa-miR-130a-5p	hsa-miR-329-5p
hsa_circ_0000745	up	hsa-miR-9-5p	hsa-miR-145-5p	hsa-miR-526b-5p	hsa-miR-578	hsa-miR-29a-5p
hsa_circ_0070113	up	hsa-miR-103a-3p	hsa-miR-107	hsa-miR-615-3p	hsa-miR-486-3p	hsa-miR-301a-5p
hsa_circ_0005383	up	hsa-miR-2113	hsa-miR-367-5p	hsa-miR-432-5p	hsa-miR-15a-3p	hsa-miR-506-3p
hsa_circ_0045372	up	hsa-miR-188-5p	hsa-miR-298	hsa-miR-485-5p	hsa-miR-216a-3p	hsa-miR-598-5p
hsa_circ_0049487	up	hsa-miR-138-5p	hsa-miR-495-5p	hsa-miR-373-5p	hsa-miR-500a-3p	hsa-miR-1296-3p
hsa_circ_0067175	up	hsa-miR-624-5p	hsa-miR-300	hsa-miR-377-3p	—	—
hsa_circ_0007934	Down	hsa-miR-498	hsa-miR-22-5p	hsa-miR-367-5p	hsa-miR-708-5p	hsa-miR-34a-5p
hsa_circ_0001818	Down	hsa-miR-17-3p	hsa-miR-433-3p	hsa-miR-367-5p	hsa-miR-335-3p	hsa-miR-642a-5p
hsa_circ_0079619	Down	hsa-miR-541-5p	hsa-miR-486-3p	hsa-miR-888-3p	hsa-miR-140-5p	hsa-miR-623
hsa_circ_0008305	Down	hsa-miR-545-5p	hsa-miR-381-5p	hsa-miR-147a	hsa-miR-429	hsa-miR-200b-3p
hsa_circ_0062937	Down	hsa-miR-378a-3p	hsa-miR-378d	hsa-miR-519d-5p	hsa-miR-526b-5p	hsa-miR-29a-5p
hsa_circ_0011692	Down	hsa-miR-133a-3p	hsa-miR-133b	hsa-miR-185-5p	hsa-miR-424-5p	hsa-miR-149-5p
hsa_circ_0018909	Down	hsa-miR-627-3p	hsa-miR-199b-5p	hsa-miR-450b-3p	hsa-miR-769-3p	hsa-miR-154-5p
hsa_circ_0055412	Down	hsa-miR-661	hsa-miR-612	hsa-miR-146b-3p	hsa-miR-484	hsa-miR-762
hsa_circ_0012967	Down	hsa-miR-105-5p	hsa-miR-181d-5p	hsa-miR-515-5p	hsa-miR-567	hsa-miR-96-3p
hsa_circ_0049888	Down	hsa-miR-138-5p	hsa-miR-570-5p	hsa-let-7g-3p	hsa-miR-372-5p	hsa-miR-588

binding sites are present on circRNAs to regulate the miRNA target gene. Previous research has shown that circRNAs play a key role in regulation of gene expression of target miRNAs; high levels of circRNA expression result in upregulation of miRNA target gene expression, while low circRNA expression causes downregulation of miRNA target gene expression. The multiple miRNA binding sites of circRNAs can instantly engage or release large amounts of miRNAs. Thus, the binding capacity of circRNAs is likely to be affected by storage and remote delivery of miRNAs.

The antisense sequence to the cerebellar degeneration-related protein 1 transcript (CDR1as) is a natural cyclic antisense transcript, which contains approximately 70 miR-7 binding sites and is not easily degraded by the RNA-induced silencing complexes (RISC), a natural inhibitor of miR-7, and plays a role in negative regulation and is known as a miRNA sponge. Some studies have indicated that CDR1as can be combined effectively with miR-7 to reduce the activity of highly expressed miR-7, resulting in increased expression levels of miR-7 target genes. This function is consistent with the competing endogenous RNA hypothesis. Furthermore, miR-7 is highly expressed in the nervous tissue and pancreas, which are associated with Alzheimer's and Parkinson's diseases through the regulation of α -synuclein and ubiquitin-protein ligase A [33,34]. CircRNA-CDR1as, as a sponge for miR-7, also has potential value in monitoring the progression of these diseases. Circular antisense non-coding RNA in the INK4 family of cyclin-dependent kinase inhibitors (CKIs) locus (cANRIL) is the cyclic antisense transcript of INK4/ARF (cyclin-dependent kinase 4 inhibitor/alternative reading frame). cANRIL can affect the inhibition of INK4a/ARF mediated by PcG (polycomb group), thus affecting the risk of atherosclerosis [35]. SRY is a sex-determining region gene of Y that contains only one exon. During embryonic development, the SRY transcription product RNA molecule exists in a linear form and provides a template for protein synthesis. However, in the adult testis, the transcription product is mainly a non-coding circRNA transcript containing approximately 16 miR-138 binding sites, that functions as a sponge for miR-138 and thus indirectly regulates the expression of target genes via inhibitory activity. MiRNAs participate in the development of pancreatic endocrine cells and insulin gene expression, secretion and utilization [36], as well as

inhibiting the expression of HIV-1 by regulating the transactivator protein via specific binding [37]. MiR-7 also functions as a tumor suppressor factor in tumorigenesis [23]. Another study showed that circRNAs may be involved the regulatory mechanisms underlying HPH (hypoxic pulmonary hypertension) [37]. These results indicate that the mechanisms of disease development related to microRNAs are indirectly related to circRNAs.

In this study, expression profiling microarray technology of human genes was used to screen differently expressed circRNAs in the plasma and PBMCs of uremic patients caused by chronic glomerulonephritis. The obtained overview of the expression of relevant circRNAs at a genome-wide level of related genes, some of which are upregulated while others are downregulated, suggests that circRNAs play a significant role in regulating the development of uremia caused by chronic glomerulonephritis. Detailed studies may clarify the molecular pathogenesis of this disease through further increase of our knowledge of the different functions of circRNAs (Table S1), and consequently improve our understanding of the mechanisms of disease associated with circRNAs, thereby improving the diagnosis and prevention of circRNA-associated diseases. An important goal is to identify a new target for intervention in molecular diagnostics and gene therapy.

Acknowledgments: This work was supported by Science and Technology Planning Project of Guangdong Province (2014A020212472), Shenzhen Science Technology and Innovation Commission (JCYJ20150403101146301).

Authors' contribution: Xi Wang and Xinzhou Zhang conceived and designed the study. Yong Dai and Wanfan Zhang performed the experiments. Xi Wang and Donglin Sun wrote the paper. Xinzhou Zhang reviewed and edited the manuscript. All authors read and approved the manuscript.

Conflict of interest disclosure: The authors declare no conflict of interest.

REFERENCES

1. Lasda E, Parker R. Circular RNAs: Diversity of form and function. *RNA*. 2014;20(12):1829-42.
2. Salzman J, Gawad C, Wang PL, Lacayo N, Brown PO. Circular RNAs are the predominant transcript isoform from hundreds of human genes in diverse cell types. *PLoS One*. 2012;7(2):e30733.

3. Memczak S, Jens M, Elefsinioti A, Torti F, Krueger J, Rybak A, Maier L, Mackowiak SD, Gregersen LH, Munschauer M, Loewer A, Ziebold U, Landthaler M, Kocks C, le Noble F, Rajewsky N. Circular RNAs are a large class of animal RNAs with regulatory potency. *Nature*. 2013;495(7441):333-8.
4. Wang Z. Not just a sponge: new functions of circular RNAs discovered. *Sci China Life Sci*. 2015;58(4):407-8.
5. Perriman R, Ares M Jr. Circular mRNA can direct translation of extremely long repeating-sequence proteins in vivo. *RNA*. 1998;4(9):1047-54.
6. Zhang Y, Zhang XO, Chen T, Xiang JF, Yin QF, Xing YH, Zhu S, Yang L, Chen LL. Circular intronic long noncoding RNAs. *Mol Cell*. 2013;51(6):792-806.
7. Baldwin DS. Chronic glomerulonephritis: nonimmunologic mechanisms of progressive glomerular damage. *Kidney Int*. 1982;21(1):109-20.
8. Zhu XJ, Niu F, Liu Y, Xu CY, Guo HJ. Pathogeny analysis of 2011 chronic renal failure patients. *Zhonghua Jian Yan Yi Xue Za Zhi*. 2014(11):1770-2. Chinese
9. Bachmayr-Heyda A, Reiner AT, Auer K, Sukhbaatar N, Aust S, Bachleitner-Hofmann T, Mesteri I, Grunt TW, Zeillinger R, Pils D. Correlation of circular RNA abundance with proliferation--exemplified with colorectal and ovarian cancer, idiopathic lung fibrosis, and normal human tissues. *Sci Rep*. 2015;5:8057. Li P, Chen S, Chen H, Mo X, Li T, Shao Y, Xiao B, Guo J. Using circular RNA as a novel type of biomarker in the screening of gastric cancer. *Clin Chim Acta*. 2015;444:132-6.
10. Qin M, Liu G, Huo X, Tao X, Sun X, Ge Z, Yang J, Fan J, Liu L, Qin W. Hsa_circ_0001649: A circular RNA and potential novel biomarker for hepatocellular carcinoma. *Cancer Biomark*. 2016;16(1):161-9.
11. Bachmayrheyda A, Reiner AT, Auer K, Sukhbaatar N, Aust S, Bachleitnerhofmann T, Mesteri I, Grunt TW, Zeillinger R, Pils D. Correlation of circular RNA abundance with proliferation--exemplified with colorectal and ovarian cancer, idiopathic lung fibrosis, and normal human tissues. *Sci Rep*. 2015;5:8057.
12. Kuo CC, Lin SC. Altered FOXO1 transcript levels in peripheral blood mononuclear cells of systemic lupus erythematosus and rheumatoid arthritis patients. *Mol Med*. 2007;13(11-12):561-6.
13. Lasagni L, Ballerini L, Angelotti ML, Parente E, Sagrinati C, Mazzinghi B, Peired A, Ronconi E, Becherucci F, Bani D, Gacci M, Carini M, Lazzeri E, Romagnani P. Notch activation differentially regulates renal progenitors proliferation and differentiation toward the podocyte lineage in glomerular disorders. *Stem Cells*. 2010;28(9):1674-85.
14. Murea M, Park JS, Kato H, Gruenwald A, Niranjana T, Si H, Thomas DB, Pullman JM, Melamed ML, Susztak K. Expression of Notch pathway proteins correlates with albuminuria, glomerulosclerosis, and renal function. *Kidney Int*. 2010;78(5):514-22.
15. Sassi C, Guerreiro R, Gibbs R, Ding J, Lupton MK, Troakes C, Lunnon K, Al-Sarraj S, Brown KS, Medway C, Lord J, Turton J, Mann D, Snowden J, Neary D7, Harris J, Bras J, ARUK Consortium, Morgan K, Powell JF, Singleton A, Hardy J. Exome sequencing identifies 2 novel presenilin 1 mutations (p.L166V and p.S230R) in British early-onset Alzheimer's disease. *Neurobiol Aging*. 2014;35(10):2422. e13-6. Kurokawa K, Akaike Y, Masuda K, Kuwano Y, Nishida K, Yamagishi N, Kajita K, Tanahashi T, Rokutan K. Down-regulation of serine/arginine-rich splicing factor 3 induces G1 cell cycle arrest and apoptosis in colon cancer cells. *Oncogene*. 2014;33(11):1407-17.
16. Kim YS, Kang HS, Herbert R, Beak JY, Collins JB, Grisom SF, Jetten AM. Kruppel-like zinc finger protein Glis2 is essential for the maintenance of normal renal functions. *Mol Cell Biol*. 2008;28(7):2358-67.
17. Hung TW, Liou JH, Yeh KT, Tsai JP, Wu SW, Tai HC, Kao WT, Lin SH, Cheng YW, Chang HR. Renal expression of hypoxia inducible factor-1 α in patients with chronic kidney disease: a clinicopathologic study from nephrectomized kidneys. *Indian J Med Res*. 2013;137(1):102-10.
18. Zhang XO, Wang HB, Zhang Y, Lu X, Chen LL, Yang L. Complementary sequence-mediated exon circularization. *Cell*. 2014;159(1):134-47.
19. Memczak S, Jens M, Elefsinioti A, Torti F, Krueger J, Rybak A, Maier L, Mackowiak SD, Gregersen LH, Munschauer M, Loewer A, Ziebold U, Landthaler M, Kocks C, le Noble F, Rajewsky N. Circular RNAs are a large class of animal RNAs with regulatory potency. *Nature*. 2013;495(7441):333-8.
20. Jeck WR, Sorrentino JA, Wang K, Slevin MK, Burd CE, Liu J, Marzluff WF, Sharpless NE. Circular RNAs are abundant, conserved, and associated with ALU repeats. *RNA*. 2013;19(2):141-57.
21. Hansen TB, Jensen TI, Clausen BH, Bramsen JB, Bente F, Damgaard CK, Kjems J. Natural RNA circles function as efficient microRNA sponges. *Nature*. 2013;495(7441):384-8.
22. Lee H, Lee JC, Kwon JH, Kim KC, Cho MS, Yang YS, Oh W, Choi SJ, Seo ES, Lee SJ, Wang TJ, Hong YM. The effect of umbilical cord blood derived mesenchymal stem cells in monocrotaline-induced pulmonary artery hypertension rats. *J Korean Med Sci*. 2015;30(5):576-85.
23. Dong S, Xiong W, Yuan J, Li J, Liu J, Xu X. MiRNA-146a regulates the maturation and differentiation of vascular smooth muscle cells by targeting NF- κ B expression. *Mol Med Rep*. 2013;8(2):407-12.
24. Neal CS, Michael MZ, Pimlott LK, Yong TY, Li JY, Gleadle JM. Circulating microRNA expression is reduced in chronic kidney disease. *Nephrol Dial Transplant*. 2011;26(11):3794-802.
25. Lu J, Kwan BC, Lai FM, Tam LS, Li EK, Chow KM, Wang G, Li PK, Szeto CC. Glomerular and tubulointerstitial miR-638, miR-198 and miR-146a expression in lupus nephritis. *Nephrology (Carlton)*. 2012;17(4):346-51.
26. Tian SL, Jiang H, Shi J. TRPM7: a membrane protein with ion channel and kinase activities. *Progress in Physiology*. 2009;40(3):253-7.
27. Liang JB, Cheng XW, Miao SY, Wang LF. Expression, purification of testis specifically expressed protein RNF138 and antibody preparation against RNF138. *Journal of Henan Normal University*. 2011;39(3):111-4. Sassi C, Guerreiro R, Gibbs R, Ding J, Lupton MK, Troakes C, Lunnon K, Al-Sarraj S, Brown KS, Medway C, Lord J, Turton J, Mann D, Snowden J, Neary D, Harris J, Bras J; ARUK Consortium,

- Morgan K, Powell JF, Singleton A, Hardy J. Exome sequencing identifies 2 novel presenilin 1 mutations (p.L166V and p.S230R) in British early-onset Alzheimer's disease. *Neurobiol Aging*. 2014;35(10):2422.e13-6. Enright AJ, John B, Gaul U, Tuschl T, Sander C, Marks DS. MicroRNA targets in *Drosophila*. *Gen Biol*. 2003;5(1):R1.
28. Pasquinelli AE. MicroRNAs and their targets: recognition, regulation and an emerging reciprocal relationship. *Nat Rev Genet*. 2012;13(4):271-82.
 29. Bingol B, Sheng M. Deconstruction for reconstruction: the role of proteolysis in neural plasticity and disease. *Neuron*. 2011;69(1):22-32.
 30. Lonskaya I, Shekoyan AR, Hebron ML, Desforgues N, Algarzae NK, Moussa CE. Diminished Parkin Solubility and Co-Localization with Intraneuronal Amyloid- β are Associated with Autophagic Defects in Alzheimer's Disease. *J Alzheimers Dis*. 2013;33(1):231-47.
 31. Burd CE, Jeck WR, Yan L, Sanoff HK, Zefeng W, Sharpless NE. Expression of linear and novel circular forms of an INK4/ARF-associated non-coding RNA correlates with atherosclerosis risk. *PLoS Genet*. 2010;6(12):e1001233.
 32. Yuan-Yuan J, Jian-Feng W, Xue-Jun W, Li Y. Roles of Non-coding RNA in Pancreatic islet development and functioning. *Zhongguo Yi Xue Ke Xue Yuan Xue Bao*. 2014;36(6):691-6. Chinese.
 33. Xia SJ, Tai XT, Li B, Luo JY, Di H, Liu LM, Wan WB, Hu MD. Study of circular RNA expression profile of lungs in the mice with hypoxia-induced pulmonary hypertension. *Chinese Journal of lung Disease*. 2015(1):34-8. Chinese.

Supplementary Table

Table S1. The function of verified circRNAs

circRNA name	Regulation	Gene and function
hsa_circ_0037409	up	TSC2: tumor suppressor gene, induce kidney damage and associated with cardiovascular disease.
hsa_circ_0044922	up	USP32: ubiquitin and ubiquitin-like (Ubl) proteins, associated with cardiovascular disease and regulate various cellular processes.
hsa_circ_0004951	up	TRPM7: participates in the regulation of the renal microcirculation.
hsa_circ_0049271	down	KEAP1: transcription factor that binds to the antioxidant response element.
hsa_circ_0053958	down	CRIM1: associated with renal fibrosis.
hsa_circ_0000369	down	Fli-1: the transcription factor of cell development.
hsa_circ_0101521	up	TRPM7: participates in the renal tubular ion transport, renal microcirculation.
hsa_circ_0101364	up	HIF1A: hypoxia induced factor, associated with inflammatory infiltrates, fiber ring, and stromal hyperplasia.
hsa_circ_0103218	up	BMPR2: similar as uremic toxins.
hsa_circ_0102682	down	CRIM1: associated with organ development, renal fibrosis.
hsa_circ_0102750	down	MEIS1: associated with restless legs.
hsa_circ_0102075	down	BMP1: osteoblast differentiation, renal osteodystrophy